Zagazig University Medical Journal
www.zumj.journals.ekb.eg
https://doi.org/10.21608/zumj.2024.234154.2873 Volume 30, Issue 1.7, Oct. 2024, Supplement Issue
Manuscript ID: ZUMJ-2204-2546 (R3) Doi: 10.21608/ZUMJ.2022.132439.2546
ORIGINAL ARTICLE

Resveratrol Ameliorates Hydroxychloroquine-Induced Retinopathy by Autophagy Induction: Molecular and Morphological Evidences

Karima F. Abdelfadeel[1],Omaima I. Abdel Hamid[2], Zeinab M. Alazouny[1*]
[1]Histology and Cell Biology Department, [2]Forensic Medicine & Clinical Toxicology Department,Faculty of Medicine, Zagazig University, Egypt.

1Histology and Cell Biology Department, Faculty of Medicine, Zagazig University, Egypt.
2Forensic Medicine and Clinical Toxicology Department, Faculty of Medicine, Zagazig University, Egypt.

Corresponding author*
Zeinab M. Alazouny

E-mail:
dr.zeinab_alazouny@yahoo.com

Submit Date 09-04-2022
Revise Date 19-04-2022
Accept Date 23-04-2022

ABSTRACT

Background: Hydroxychloroquine (HCQ) has been utilized globally for about 75 years initially as an antimalarial drug, however, its uses expanded to include autoimmune diseases. It is being investigated for its potential to treat coronavirus disease. The widespread use and self-treatment led to concerns of potential harm from toxicities. Retinopathy is considered the major dose-limiting toxicity of HCQ. **Aim of Work:** to explore the potential ameliorative effect of resveratrol on HCQ-induced retinopathy in rats. **Methods:** Fifty adult male rats were randomly assigned to 3 groups, control, HCQ-treated group received hydroxychloroquine sulfate 62mg/kg/day HCQ&resveratrol-treated group treated with hydroxychloroquine sulfate 62mg/kg/day, and the resveratrol 20mg/kg/day. After the termination of 12 weeks of dosing, the serum of rats was used for estimation of caspase-3, tumor necrosis factor-alpha (TNF-α), oxidative stress parameters malondialdehyde (MDA), protein carbonyl, 8-hydroxy-2′-deoxyguanosine (8-OHdG) and total antioxidant capacity (TAC). The rats were sacrificed and retinas were isolated for detection of gene expression of mammalian target of rapamycin (mTOR), Microtubule-Associated Protein-1 Light Chain-3 (LC3B), Beclin-1, and p62 using qRT-PCR, histopathological, ultrastructural and immunohistochemical expression of Bcl-2. **Results:** HCQ treatment led to significant increase in caspase-3, TNF-α, (MDA), protein carbonyl, and 8-OHdG with significantly decreased TAC. The significantly increased expression of mTOR led to autophagy inhibition manifested as a significant reduction of LC3B, Beclin-1 expression, and a significantly increased p62 expression. There were many retinal pathological changes including decreased retinal thickness with disorganization, vaculation, pyknosis, and diminished cell population.**Conclusions:** Concurrent treatment with resveratrol induced an obvious improvement in retinal pathology through antioxidant and autophagy-inducing effects.

Keywords: resveratrol, hydroxychloroquine, retinopathy, autophagy mTOR

INTRODUCTION

Initially, Hydroxychloroquine (HCQ) had been utilized for decades as an antimalarial drug but it has now become universally the mainstay in the management of certain chronic inflammatory diseases mainly, systemic lupus erythematosus (SLE) and rheumatoid arthritis[1]. It is similarly used in the treatment of additional rheumatic disorders, involving dermatomyositis, cutaneous lupus, undifferentiated connective tissue disorders, and seronegative inflammatory arthritis[2].

Hydroxychloroquineis being assessed to prevent and cure coronavirus-2019 (COVID-19) disease. There is limited high-quality evidence that such use is beneficial, in addition to raising concerns about potential harm from side effects and toxicities[3].The standard therapeutic dose of hydroxychloroquine is 400 mg/d[4].

Retinopathy that can induce vision loss is considered the key dose-limiting toxicity of HCQ. The use of advanced highly sensitive screening techniques that can recognize earlier grades of retinopathy resulted in the identification of a considerably higher prevalence of HCQ-induced retinopathy than was previously documented. The total prevalence of retinopathy in patients under HCQ therapy for longer than 5 years was found to be 7.5 percent, rising to nearly 20 percent after 20 years of therapy[5].

Screening for HCQ-induced retinopathy can reveal structural or functional alterations in the macula before symptoms or fundus abnormalities arise[6] Unfortunately, Moschos et al. reported that drug cessation in early HCQ-induced retinopathy improves visual function but doesn't improve the structural parameters including retinal thickness[7].

Resveratrol (3,5,4-trihydroxystilbene) is a natural polyphenol non-flavonoid micronutrient product that is found in different foods with different concentrations such as grape, mulberry, cranberry, and peanut[8]. Aggarwal et al. reported that resveratrol is considered as an antitoxin which is produced by at least 72 medicinal and edible plant species in response to a variety of environmental stressors including invading fungal infection, excessive sunlight, and ultraviolet radiation. Resveratrol has gained great interest due to its numerous health benefits[9]

Resveratrol possesses a wide range of biological actions, including antioxidant and anti-inflammatory effects. In the last two decades, its cancer-preventive and anti-cancer properties, as well as its role in pain, inflammation, tissue injury, and other diseases, have indeed attracted much interest[10]. The molecular targets and signaling pathways affected by resveratrol are many and involve the mTOR and NF-κB pathways. Resveratrol might have numerous additional targets e.g.: cyclooxygenase (COX), phosphodiesterases (PDEs), Phosphatidylinositol-3-Kinase (PI3K), and p70 S6 kinase (p70S6K)[11].

Previous research has suggested that resveratrol is a natural autophagy regulator that can induce autophagy in different cancers and can be used both for cancer chemoprevention and therapy[12].Resveratrol can be also used to prevent and treat Alzheimer's disease, and other

neurodegenerative diseases as epilepsy, Parkinson's disease, Huntington's disease, amyotrophic lateral sclerosis, and nerve injury[13].

However, few studies examined the effect of resveratrol on HCQ-induced retinopathy. So, the current work aims to examine the effects of resveratrol on HCQ-induced retinopathy in adult albino male rats.

METHODS

chemicals

(1) Hydroxychloroquine Sulfate (HCQ): was purchased from Sigma-Aldrich in the form of off-white powder.

(2) Resveratrol: Resveratrol (Mega Resveratrol®), 99 % pure pharmaceutical grade, was obtained from Mega Resveratrol and Candlewood Stars Inc., Danbury, USA

Animals

Fifty male adult (12±1 week) albino rats with a weight ranging from 280 to 320 gm were purchased from the animal house of Faculty of Medicine- Zagazig University, Egypt and used in the current work. Before the start of the study, the rats were given a 14-day period of passive elimination to eliminate diseased animals, assess their physical well-being, and acclimate them to the new conditions. The rats were kept in plastic cages away from any chemical contamination in standard laboratory conditions which include 22±2^{o}C ambient temperature, 50±5% humidity and a 12 hours light–dark cycle. They were offered food and water ad Libitum in equal quantities to all rats.

The rats received care by the standards of the National Guide for Care and Use of Laboratory Animals (NIH Publications No. 8023, revised 1978). The study design was approved by the Institutional Animal Care and Use Committee (IACUC), Zagazig University, Egypt.

The experiment complies with the ARRIVE guidelines (Animal Research: Reporting of In Vivo Experiments) and is carried out by the U.K. animal experiments

Study protocol:

The study extended for 12 weeks, the rats were randomly divided into three groups:

- Group (I); control group: 30 rats, they were further subdivided into
  - Group (Ia); negative control group: 10 rats that were kept without intervention aiming to estimate the basic parameters.
  - Group (Ib); positive control group: 10 rats, each rat was treated with 1ml distilled water/day by oral gavage.
  - Group (1c); Resveratrol-treated group (RES-treated group): 10 rats, each received resveratrol 20 mg/kg/day dissolved in 1 ml distilled water by oral gavage.[14]
- Group (II); hydroxychloroquine-treated group (HCQ-treated group): 10 rats, each was treated with hydroxychloroquine sulfate 62 mg/kg/day (1/20 LD50) dissolved in 1 ml distilled water by oral gavage.[15]
- Group (III); hydroxychloroquine and resveratrol-treated group (HCQ&RES-treated group): 10 rats; each was treated with a combination of hydroxychloroquine and resveratrol in the same previous doses.

At the end of the treatment period, all rats were exposed to:

- Biochemical analysis:

Rats were anesthetized and blood samples were obtained from the retro-orbital plexus through the use of capillary glass tubes following the method described by van Herck et al [16] The samples were allowed for spontaneous coagulation, then centrifuged for 10 minutes at 3000 r.p.m to separate sera that were stocked at -20^{o}C for estimation of:

- Caspase-3 level:

It was estimated using caspase 3 (Casp-3) rat ELISA kit (Cat Number CSB-E08857r) from Cusabio Technology, China. The test utilizes the quantitative sandwich enzyme immunoassay. The amount of Casp-3 in the sample (ng/ml) is proportional to the intensity of the color developed which is measured at 450 nm

- Tumor necrosis factor-alpha (TNF-α):
  It was estimated using a rat TNF-α ELISA kit (Cat Number CSB-E11987r) from Cusabio Technology, China. The test uses the quantitative sandwich enzyme immunoassay. The amount of TNF-α in the sample (pg/ml) is proportional to the intensity of the color developed which is measured at 450 nm
- Oxidative stress parameters {lipid, protein and DNA oxidation products (MDA, protein carbonyl, 8-OHdG)} and total antioxidant capacity (TAC)}:
  The lipid peroxidation end-product malondialdehyde (MDA) was estimated using Biodiagnostic kit (Giza, Egypt with cat. No. MD 2529) according to the kit instructions. The end-product of protein oxidation (protein carbonyl) and the DNA oxidation end-product (8-OHdG) were assayed colormetrically by the MyBioSource ELISA kit (San Diego, USA) cat. No MBS726854 and MBS269902 respectively. Serum TAC was measured using colorimetric assay kits (cat. No. E-BC-K136-S) purchased from Elabscience, USA, according to the manufacturer's protocol.

- Measurement of gene expression of mTOR, Microtubule-Associated Protein 1 Light Chain 3 (LC3B), Beclin-1, and p62 in retinal tissue using Quantitative Reverse Transcriptase-Polymerase Chain Reaction (qRT-PCR):
  Retina was isolated through a corneal incision, frozen in liquid nitrogen, and stored at a temperature of −80 °C. After adding TRIzolTM Reagent (Invitrogen, Carlsbad, CA, USA) to each rat's retinal tissue sample, it was homogenized using a tissue homogenizer. The total RNA was isolated using the RNeasy Mini Kit (Qiagen GmbH, Hilden, Germany), and the RNA purity and quantity were determined using the Agilent 2100 Bioanalyzer (Agilent Technologies, Santa Clara, CA). QiagenQuantiTect kit for Reverse Transcription (Heidelberg, Germany) was used to transcript the first-stand complementary DNA (cDNA) from the isolated mRNA. The used primers were designed by the Primer-BLAST tool (http://www.ncbi.nlm.nih.gov/tools/primer-blast) as shown in Table (1). The PCR was carried out using the QuantiTect SYBR Green PCR kits (Qiagen, Heidelberg, Germany) according to the manufacturer's instructions. 2 µl of cDNA, 0.4 µl of each primer (10 umol/µl) and 10 µl of SybrGreen qPCR Master Mix were used. The ABI 7500 Real-Time PCR system (Applied Biosystems) was used to run duplicates of all specimens. The thermal profile for the PCR reaction was as follows: denaturation for 10 min at 94C, followed by 40 cycles of 15 s at 94C, 30 s at 58C, and 40 s at 72C. The SDS 2.0.1 software (Applied Biosystems) provided by the thermal cycler manufacturer was used to determine the cycle threshold (Ct) values. β-actin was involved as a housekeeping gene and used as an internal control aiming to normalize the input load of cDNA. The $2^{-\Delta\Delta CT}$ method described by Livak and Schmittgenwas used to estimate the relative gene expression in a fold change.[17]
- Histopathological study:
  Rats were sacrificed after obtaining blood samples. Following the method described by Fielden et al.; eyes were enucleated immediately after death with taking care to

minimize trauma. Freshly enucleated eyeballs were fixed in 10% formolsaline. Aiming to guard against ischemic-hypoxic change after enucleation, the retinas were acutely dissected post-fixation for 1 hour creating a slit behind the limbus to facilitate penetration of the fixative[18], and then the retinas were processed to get 4 µm paraffin sections and stained with hematoxylin and eosin stain following the method described by Bancroft and Layton and examined by routine light microscopy.[19]

Immunohistochemical study:

For Bcl-2 detection, streptavidin biotin-peroxidase immunostaining was used consuming rat Bcl-2 polyclonal antibody purchased from MyBiosource, Inc., USA (Cat.# MBS8004797). Paraffin sections were exposed to deparaffinization and rehydration. The slices were treated with the primary antibody after suppressing endogenous peroxidase activity with 3 percent hydrogen peroxide. The secondary antibody (goat anti-rabbit IgG: HRP) was then applied after washing with phosphate buffer. The slides were then stained with Streptavidin-Biotin peroxidase, which binds to the Biotin on the secondary antibody. The immune reaction was visualized using the chromogen diaminobenzidine (DAB). Lastly, Meyer's hematoxylin was used to counterstain the slides. Brown cytoplasmic granules indicated a positive reaction. A negative control was obtained by skipping the primary antibody step, while a positive control was obtained using a section of osteocarcinoma[20]

- Transmission Electron Microscopy Study:

The eyeballs were extracted then the retinas were dissected and immediately immersed in the 2.5% cocodylate-buffered glutaraldehyde for 24 h at 4°C. They were then post-fixed for 2 hours at room temperature in 1.0 percent osmium tetroxide in 0.1 mol/l cacodylate buffer (pH 7.3). The samples were then dehydrated in ethanol that was graded in ascending order. Following three 10-minute immersions in propylene oxide, the samples were impregnated overnight in a mixture of propylene oxide and embedded in Epon-812 resin. Ultrathin sections were cut with an ultramicrotome (Leica Ultracut, Berlin, Germany) and stained with toluidine blue. 2 percent uranyl acetate and lead citrate were used to counterstain ultrathin sections[21]. Stained sections were examined and photographed using a JEOL JEM 2100 electron microscope in the Faculty of Agriculture El Mansoura University's Electron Microscope Research Laboratory.

- Morphometric study:

The full retinal thickness and the area percentage (area percent) of positive immunoreaction for Bcl-2 were calculated using a Leica Qwin 500 (Leica Ltd, Cambridge, UK) image analyzer in the Pathology Department, Faculty of Dentistry, Cairo University, Egypt. Digimizer 4.3.2 image analysis software was used to measure it from digital images scanned at x400 (MedCalc Software bvba, Belgium).

The full retinal thickness was measured in both eyes of all rats. It is calculated using linear measurements taken between the apical portion of the RPE and the outer margin of the ganglion cell layer, which was chosen to avoid the layer's inherent variability in thickness and cellularity. Comparisons to the control group were used to estimate the percentage change in mean thickness measurements for each treatment group.[18].

STATISTICAL ANALYSIS

Statistical Package for Social Science version 16 was used to manage the data after it was collected and tabulated (SPSS Inc., Chicago,

IL). They were expressed as mean ± standard deviation (SD); statistical differences among the study groups were evaluated by one-way analysis of variance (ANOVA) followed by the Turkey post-hoc test for inter-group comparisons. Statistical significance was defined as a p-value of less than 0.05.

RESULTS

Because there was no statistically significant difference in all of the estimated parameters between the control subgroups (Ia), (Ib), and (Ic), the control subgroup (Ia) was used in the statistical comparison to the other study groups.

- *Biochemical results:*

  Table (S2) showed that the mean values of serum caspase-3 and TNF-α in HCQ-treated rats were significantly higher than in control rats ($p<0.01$), while resveratrol co-treatment in group 3 resulted in a significant decline in these parameters when compared to HCQ-treated rats and they showed a non-significant difference from the control values ($p>0.05$)

  Table (S2) showed that the oxidative stress parameters in the sera of rats revealed that MDA, protein carbonyl, and 8-OHdG were significantly higher in the serum of HCQ-treated rats when compared to the control ($p<0.01$). The above-mentioned parameters are also significantly lower in the hydroxychloroquine and resveratrol-treated groups when compared to the HCQ-treated group ($p<0.01$), and they do not differ significantly from the control group. The TAC in the HCQ-treated group was significantly lower than the control ($p<0.01$), and the co-administration of hydroxychloroquine and resveratrol significantly increased the mean values of TAC when compared to the HCQ-treated groups (p0.05), but was still significantly lower than the control ($p<0.05$)

- Gene expression of mTOR, Microtubule-Associated Protein 1 Light Chain 3 (LC3B), Beclin-1, and p62 in retinal tissue:

  Rat treatment with hydroxychloroquine Sulfate in group II causes significant inhibition of autophagy manifesting as a significant reduction of the expression of LC3B and Beclin-1, and a significant increase in the expression of p62 when compared to the control group while the concurrent treatment with HCQ and resveratrol in group III resulted in reversal of this condition where the levels of expression of LC3B, beclin-1 where significantly higher and levels of expression of p62 were significantly lower from those in group II and there were non-significantly different from the control group (table S3). There was a significant increase in the mTOR expression in HCQ-treated group when compared to control and there was significantly decreased expression in HCQ and resveratrol-treated group when compared to HCQ-treated group with non-significant difference from control values.

- *Histopathological results:*

  The subgroups (a, b and c) of the control group revealed similar results. Only morphological results of subgroup 1a were presented.

  Haematoxylin and eosin-stained sections of the control group showed a normal arrangement of retinal layers: The photoreceptor layer's inner and outer segments, the outer limiting membrane (OLM), the outer nuclear layer (ONL), the outer plexiform layer (OPL), the inner nuclear layer (INL), the inner plexiform layer (IPL), the ganglion cell layer, and the inner limiting membrane (Fig. 1a). However, the HCQ-treated group showed irregular processes of photoreceptors and diminished cell population of the outer nuclear layer (ONL) with empty

Spaces between their nuclei. Areas of fusion between INL and ONL were seen. The ganglion cell layer showed vacuolations and congested capillaries. The presence of scarce ganglion cells was detected (Fig. 1b). The HCQ&RES-treated group showed a partially preserved histological structure of the retinal layers with the restoration of the cell population of the outer and inner nuclear as well as the ganglion cell layers. However, few spaces were seen between nuclei of ONL and few congested capillaries were seen in the ganglion cell layer (Fig. 1c).

Examination of H&E stained sections of the upper part of the retina of the control group showed the photoreceptor layer with an eosinophilic parallel fibrillary striation pattern. It was composed of lightly stained outer segments and deeply stained inner segments of rods and cones. The outer limiting membrane appeared as a thin membrane situated at the junction of the photoreceptor layer and the outer nuclear layer. The thick outer nuclear layer (ONL) was composed of several rows of closely packed densely stained nuclei of cell bodies of rods and cones (Fig. 2a). However, HCQ-treated group showed many vacuolations in the outer segment of photoreceptors and irregularly oriented inner segment. Also, diminished cell population of outer and inner nuclear layers was noticed with empty spaces between their cells. There were several pyknotic nuclei and some congested blood capillaries (Fig. 2b). The HCQ&RES-treated group showed a partially preserved histological structure of the retinal layers with well-oriented outer segment and inner segment of photoreceptor layer and restoration of cell population of outer and inner nuclear layers. However, few spaces were seen between nuclei of ONL (Fig. 2c)

Hematoxylin and eosin stained sections of the control group's lower retina revealed that the outer plexiform layer (OPL) appeared as a loose network of acidophilic fibers, indicating the connections between photoreceptor processes and those of neurons in the inner nuclear layer (INL). The INL appeared significantly thinner than the ONL, and its cells were larger and had brighter nuclei than the ONL's. The inner plexiform layer (IPL) appeared as a loose network of acidophilic fibers connecting the INL and the ganglion cell layer (GCL). The GCL was made up of a single discontinuous row of ganglion cells that were larger than the majority of the preceding retinal cells and had faintly colored cytoplasm and vesicular spherical or angular nuclei. Ganglion cell processes spread out to form the nerve fiber layer (NFL). Supporting fibers from Muller's cells were observed traversing the IPL, GCL, and NFL finally forming the inner limiting membrane (ILM) (Fig. 3a). Examining retinal sections from the HCQ-treated group, on the other hand, revealed that the outer plexiform layer appeared as a very thin, lightly stained zone. The (OPL) and (IPL) were found to be disorganized, with expanding gaps between their fibers. The ganglion cell layer (G) exhibited vacuolations and a decrease in the number of ganglion cells (Fig. 3b). The HCQ&RES-treated group, on the other hand, had partially maintained histological structure of the retinal layers. However, some large gaps were observed between the nuclei of the inner nuclear layer (Fig. 3c).

- *Immunohistochemical study:*

Immune-histochemical staining for Bcl2 of the control and HCQ&RES-treated groups showed a strong positive immunoreaction for Bcl2 which appeared as a deep yellow-brownish cytoplasmic coloration in

photoreceptors, outer and inner plexiform layers, and ganglion cell layers (Fig. 4a&c). However, the treated group showed a weak positive immunoreaction for Bcl2 which appeared as a pale yellow-brownish cytoplasmic coloration in photoreceptors, outer and inner plexiform layers, and ganglion cell layers (Fig 4b).

- *Electron microscopic results:*

Electron microscopic examination of the retina of the control group showed that retinal pigment epithelium cells (RPEs) had an oval euchromatic nucleus and contained melanin granules in the apical portion of the cytoplasm. Few phagosomes were detected inside the cytoplasm. Well-organized outer segments of photoreceptors were seen with narrow intersegment spaces (Fig. 5a). On the other hand, examination of the treated group showed many retinal pigment epithelium cells with an irregular nucleus. Many phagosomes were observed in their cytoplasm. The outer segments of photoreceptors were relatively disorganized with wide intersegment spaces (Fig. 5b). However, the HCQ&RES-treated group exhibited many retinal pigment epithelium cells with an oval euchromatic nucleus. Some phagosomes were present within its cytoplasm. Well-organized outer segments of photoreceptors were seen with narrow intersegment spaces (Fig. 5c).

Electron microscopic examination of the outer nuclear layer of the retina of the control group showed that it contained the cell bodies of rods and cones. Rod nucleus appeared more electron-dense than the cone nucleus and had a large central mass of heterochromatin. Narrow spaces were present between the cell bodies of Rods and Cones (Fig. 6a). In HCQ-treated group, some shrunken and irregular cell bodies and nuclei of rods and cones were seen with widening of the spaces between their cell bodies (Fig. 6b). However, HCQ&RES-treated group showed intact rods and cones nuclei with narrowing of the spaces between their cell bodies (Fig. 6c).

Electron microscopic examination of the inner nuclear layer (INL) of the retina of the control group showed that it was separated from the outer nuclear layer (ONL) by the outer plexiform layer (OPL). The INL was composed of various categories of cells; Bipolar cells which appeared polygonal in shape, located close to the OPL, and their nuclei showed heterochromatin. Horizontal cells had large and rounded nuclei with fine dispersed chromatin and prominent nucleolus. Amacrine cells had rounded electron lucent nuclei (Fig. 7a). In the HCQ-treated group, bipolar cells exhibited many cytoplasmic vacuoles. Muller cells were seen with their long processes extending between the cells of the inner nuclear layer towards the outer plexiform layer. Also, Horizontal cells and amacrine cells were observed near the inner plexiform layer (Fig. 7b). HCQ&RES-treated group showed intact cells of the inner nuclear layer with minimal cytoplasmic vacuoles in bipolar cells (Fig. 7c).

Examination of the ganglion cell layer in the control group showed cell bodies of large multipolar neurons; ganglion cells, with oval euchromatic nuclei, mitochondria and RER. Un-myelinated axons of the ganglion cells were seen in the optic nerve fiber layer. The inner limiting membrane was also noticed (Fig. 8a). HCQ-treated group, showed many ganglion cells with irregular nuclei and vacuolated cytoplasm (Fig. 8b). HCQ&RES-treated group revealed ganglion cells with euchromatic nuclei. However, some vacuoles were observed in their cytoplasm (Fig. 8c).

- *Morphometerical results*:

1- Full retinal thickness:

The mean values of full retinal thickness in HCQ-treated group showed significant reduction when compared to control group ($p<0.01$) while concurrent treatment with HCQ and resveratrol significantly increased the full retinal thickness when compared to HCQ-treated group ($p<0.01$) but still significantly lower from control ($p<0.05$).

2- Mean area % of positive immunoreaction for Bcl-2 in retinal tissue:

Table (2) shows that the mean values of area % of positive immunreaction for Bcl-2 was significantly lower in HCQ-treated group when compared to the control group ($p<0.01$), while the mean values significantly increased in hydroxychloroquine and resveratrol-treated group when compared to HCQ-treated group ($p<0.01$), and they showed non-significant difference from the control group ($p>0.05$)

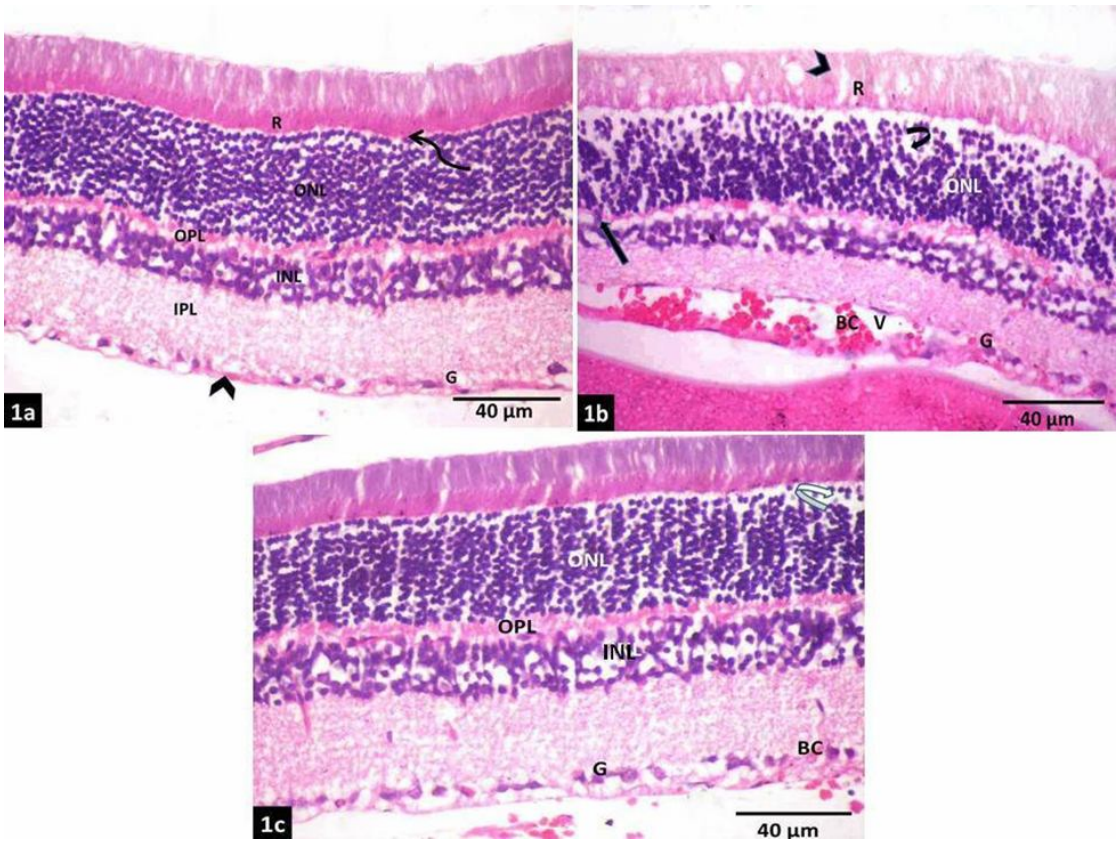

Figure 1: Photomicrographs of H&E stained sections of retina of control group (1a): showing outer and inner segments of photoreceptors (R), outer limiting membrane (spiral arrow), outer nuclear layer (ONL) formed of several rows of nuclei, outer plexiform layer (OPL), inner nuclear layer (INL), inner plexiform layer (IPL), Ganglionic cell layer (G) and inner limiting membrane (arrowhead). HCQ-treated group (1b): showing irregular processes (arrowhead) of photoreceptors (R), diminished cell population of the outer nuclear layer (ONL) with empty Spaces (curved arrow) between their nuclei. Areas of fusion between INL and ONL (arrow) are seen. The ganglion cell layer shows vacuolations (v) and congested capillaries (BC). Note the presence of a few ganglion cells (G). HCQ&RES-treated group (1c): showing a partially preserved histological structure of the retinal layers with restoration of the cell population of the outer (ONL) and inner nuclear (INL) as well as the ganglion cell (G) layers. However, few spaces are seen between nuclei of ONL (curved arrow) and few congested capillaries (BC) are seen in the ganglion cell layer (G) (H and E, X400, scale bar 40 µm).

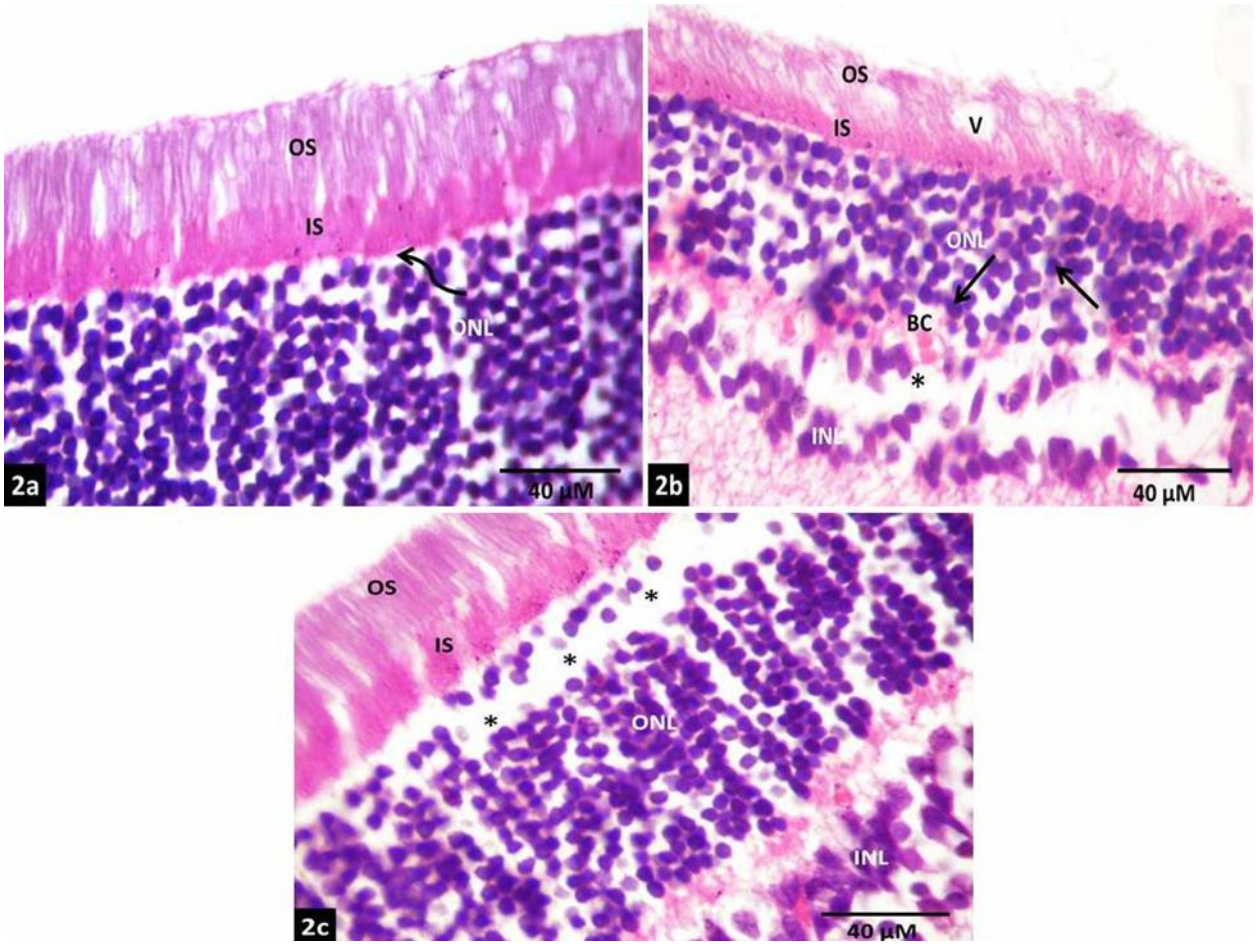

Figure 2. Photomicrographs of H&E stained sections of retina of: control group (2a): showing the photoreceptor layer with an eosinophilic parallel fibrillary striation pattern and is composed of lightly stained outer segments (OS) and deeply stained inner segments (IS) of the rods and cones. The outer limiting membrane (spiral arrow) is a thin membrane located at the junction between the photoreceptor layer and the outer nuclear layer. The thick outer nuclear layer (ONL) is composed of several rows of closely packed densely stained nuclei of cell bodies of rods and cones. HCQ-treated group (2b): showing vacuolations (v) in the outer segment (OS) of photoreceptors and irregularly oriented inner segment (IS), diminished cell population of outer (ONL) and inner nuclear layers (INL) with empty spaces between their cells (asterisk). Many pyknotic nuclei are seen (arrow). Some congested blood capillaries (BC) are seen. HCQ&RES-treated group (2c): showing partially preserved histological structure of the retinal layers with well oriented outer segment (OS) and inner segment (IS) of photoreceptor layer and restoration of cell population of outer (ONL) and inner nuclear layers (INL). However, few spaces (asterisk) are seen between nuclei of ONL (H and E, X1000, scale bar 40 µm).

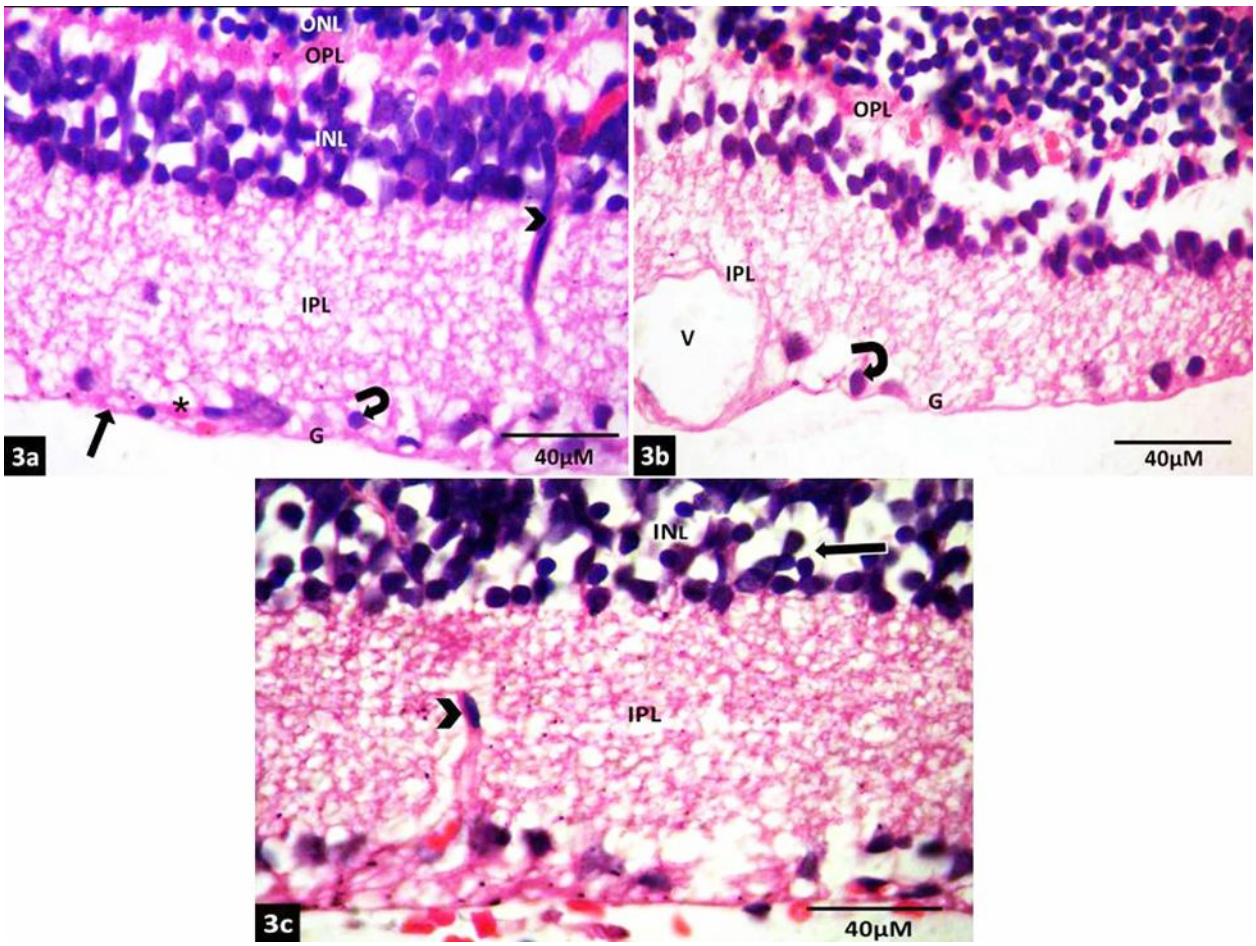

Figure 3: Photomicrographs of H&E stained sections of retina of: control group (3a): showing that the outer plexiform layer (OPL) appears as a loose reticular layer between the ONL and the INL. The INL appears much thinner than ONL and its cells are larger and contain paler nuclei than those of the ONL. A muller cell nucleus (arrow head) is seen traversing the inner plexiform layer (IPL) that has an eosinophilic fibrillary appearance and appears much thicker than OPL. The ganglion cell layer (G) is composed of a single discontinuous row of large cell bodies (curved arrow) with lightly stained cytoplasm and vesicular or angular nuclei. Axons of ganglion cells extend to form nerve fiber layer (asterisk) that is lined by inner limiting membrane (arrow). HCQ-treated group (3b): showing that the outer plexiform layer (OPL) appears as a very thin lightly stained zone. Disorganization of the (OPL) and the inner plexiform (IPL) layers and widening of spaces between their fibers are noticed. The ganglion cell layer (G) shows vacuolations (V) and diminished number of ganglion cells (curved arrow). HCQ&RES-treated group (3c): showing partially preserved histological structure of the retinal layers. However, some wide spaces (arrow) are seen between nuclei of (INL). A muller cell nucleus (arrow head) is seen traversing (IPL) (H and E, X1000, scale bar 40 µm).

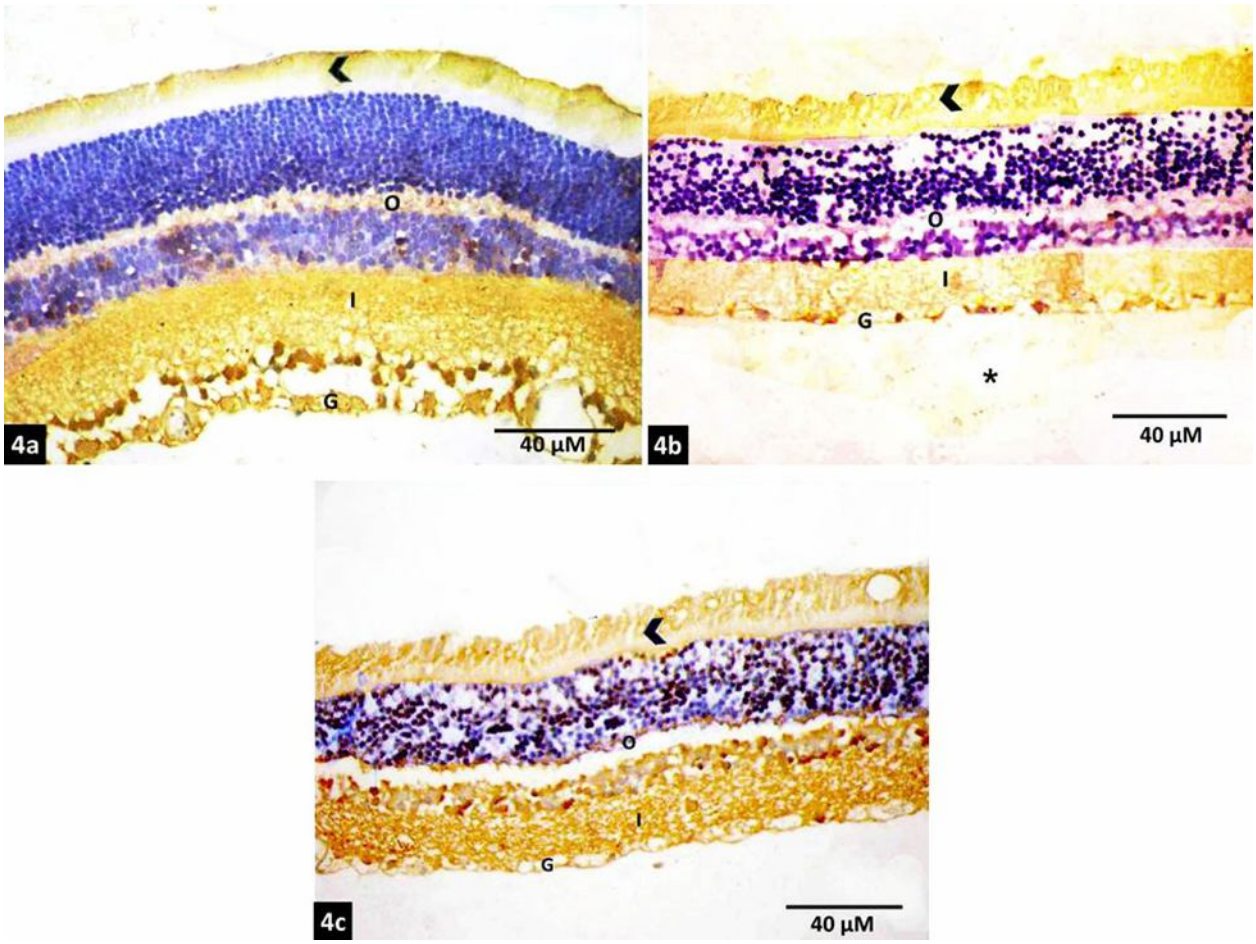

Figure 4: Photomicrographs of Bcl2 immunohistochemical stained sections of retina of: control group (4a): showing a strong positive immunoreaction for Bcl2 which appeared as deep yellow brownish cytoplasmic coloration photoreceptors (arrow head), outer (O) and inner (I) plexiform layers and ganglion cell layers (G). HCQ-treated group (4b): a weak positive immunoreaction for Bcl2 which appeared as a pale yellow brownish cytoplasmic coloration in photoreceptors (arrow head), outer (O) and inner (I) plexiform layers and ganglion cell layers (G). HCQ&RES-treated group (4c): showing a strong positive immunoreaction for Bcl2 which appeared as a deep yellow brownish cytoplasmic coloration photoreceptors (arrow head), outer (O) and inner (I) plexiform layers and ganglion cell layers (G). (Bcl2 immunostaining, X400, scale bar 40 µm).

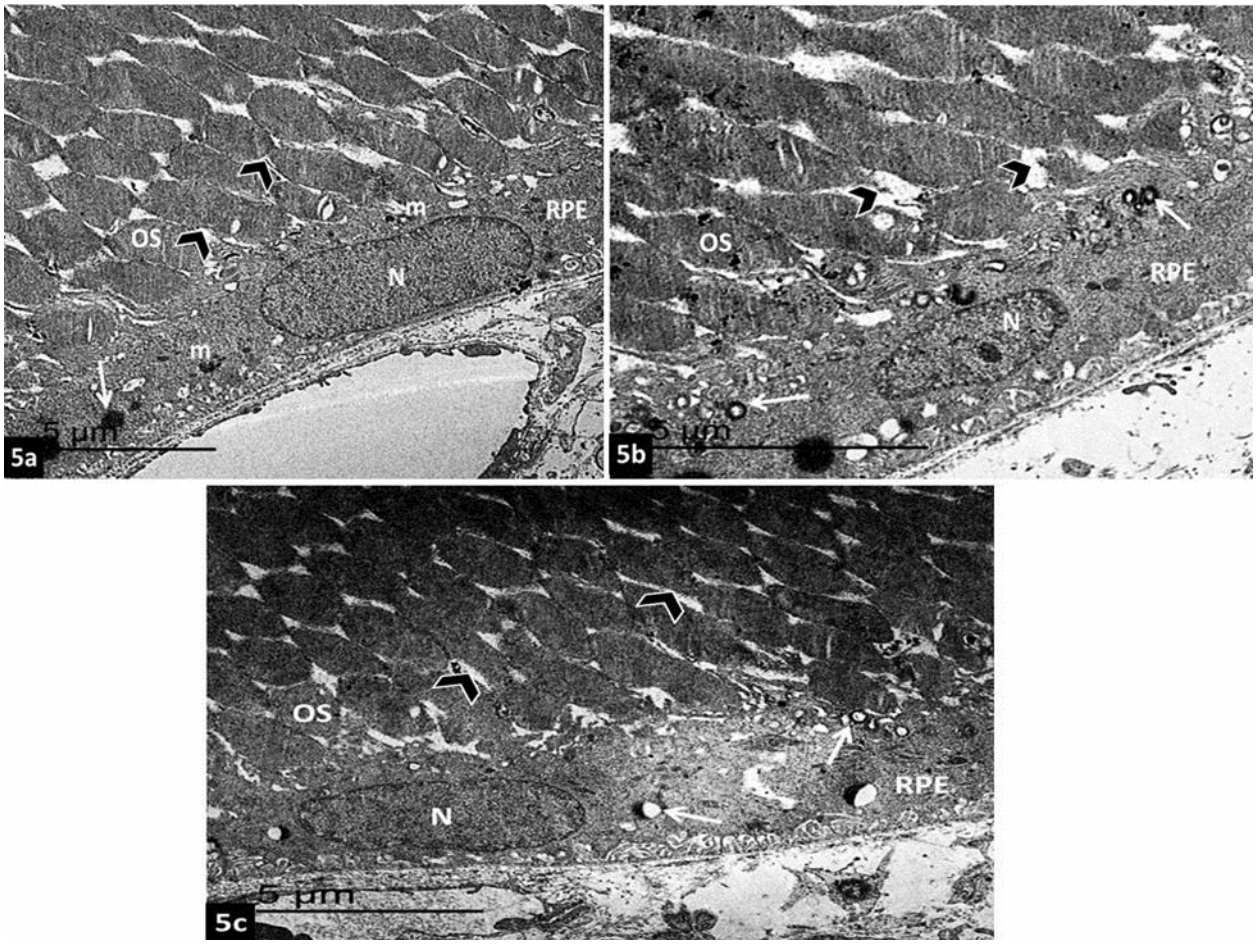

Figure 5: Electron micrographs of the retina of: the control group (5a): showing a retinal pigment epithelium cell (RPE) with an oval euchromatic nucleus (N) and contains melanin granules (m) in the apical portion of its cytoplasm. Few phagosomes (arrow) are seen in its cytoplasm. Well organized outer segments of photoreceptors (OS) are seen with narrow intersegment spaces (arrowhead) (TEMx8000, scale bar 5 µm). HCQ-treated group (5b): showing a retinal pigment epithelim cell (RPE) with an irregular nucleus (N). Its cytoplasm contains many phagosomes (arrow). The outer segments (OS) of photoreceptors are relatively disorganized with wide intersegment spaces (arrow head). (TEMx12000, scale bar 5 µm). HCQ&RES-treated group (5C): showing a retinal pigment epithelium cell (RPE) with an oval euchromtic nucleus (N). Some phagosomes (arrow) are seen within its cytoplasm. Well organized outer segments of photoreceptors (OS) are seen with narrow intersegment spaces (arrow head) (TEMx8000, scale bar 5 µm).

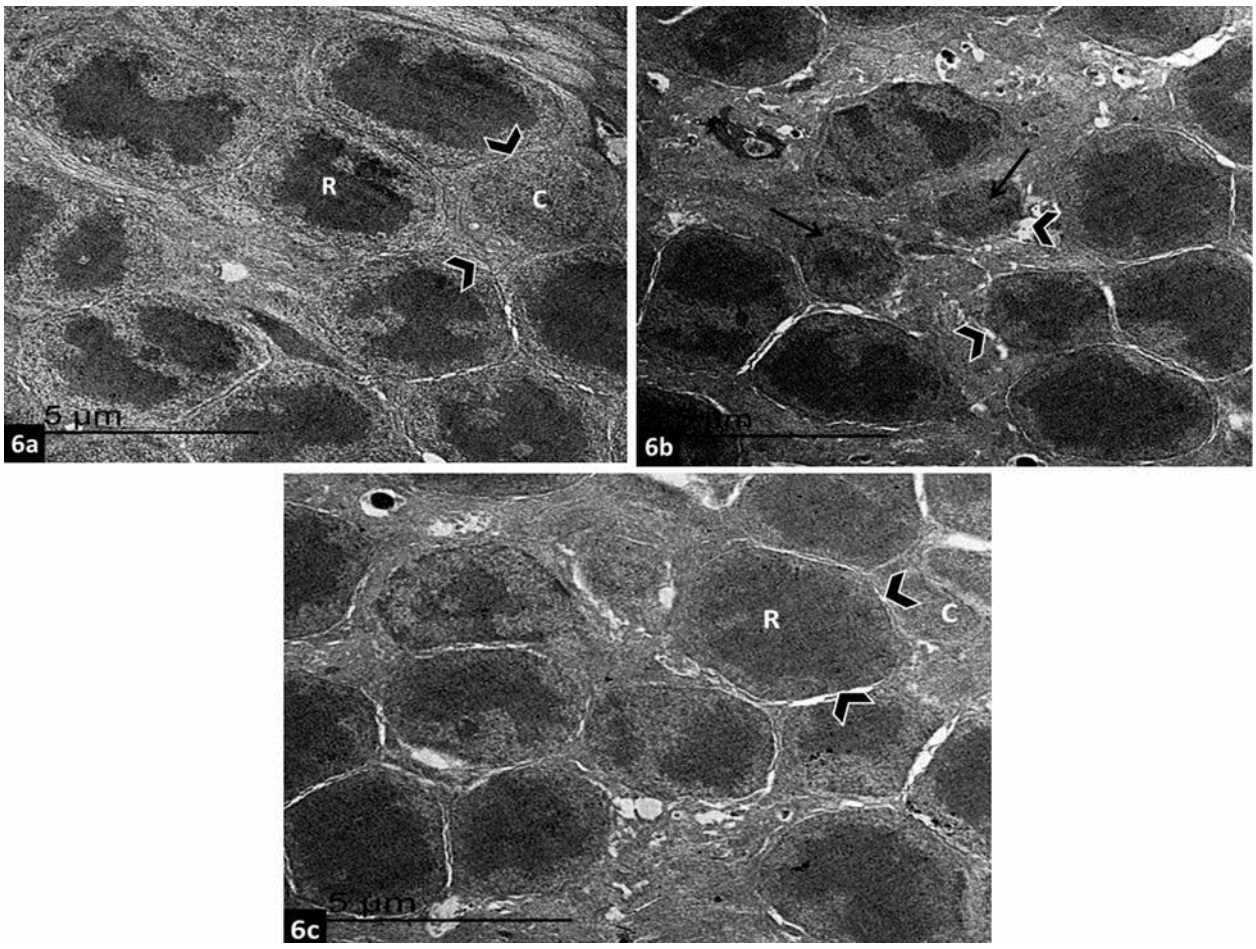

Figure 6: Electron micrographs of the outer nuclear layer of retina of: the control group (6a): showing the cell bodies of rods (R) and cones (C). Rod nucleus is more electron-dense than the cone nucleus and has a large central mass of heterochromatin. Narrow spaces (arrowhead) are present between the cell bodies of Rods and Cones (TEMx9400, scale bar 5 µm). HCQ-treated group (6b): showing shrunken and irregular cell bodies and nuclei of rods and cones (arrow) and widening of the spaces (arrowhead) between their cell bodies (TEMx9400, scale bar 5 µm). HCQ&RES-treated group (6C): showing intact rods (R) and cones (C) nuclei with narrowing of the spaces (arrowhead) between their cell bodies (TEMx9400, scale bar 5 µm).

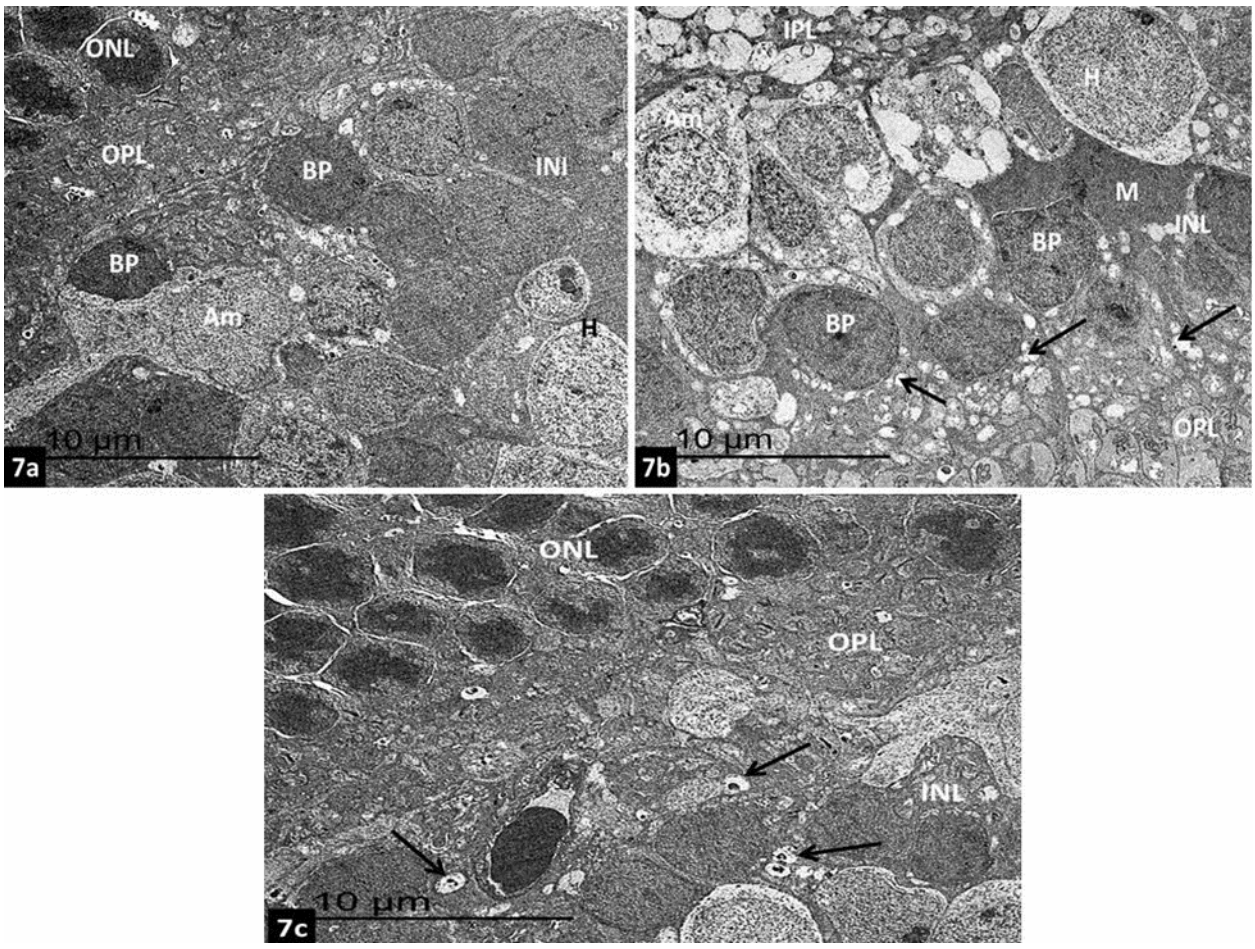

Figure 7: Electron micrographs of the inner nuclear layer of retina of: control group (7a): showing that the inner nuclear layer (INL) is formed of many types of cells separated from the outer nuclear layer (ONL) by the outer plexiform layer (OPL). Bipolar cells (BP) appear polygonal in shape close to the OPL and their nuclei show heterochromatin. Horizontal cells (H) have large and rounded nuclei with fine dispersed chromatin and prominent nucleolus. Amacrine cells (Am) have rounded electron lucent nuclei (TEMx4700, scale bar 10 µm). HCQ-treated group (7b): showing bipolar cells (BP) with many cytoplasmic vacuoles (arrow). A Muller cell (M) is seen with long processes extending between cells of inner nuclear layer (INL) towards the outer plexiform (OPL) layer. Also, Horizontal cells (H) and amacrine cells (Am) are seen towards the inner plexiform layer (IPL) (TEMx4700, scale bar 10 µm). HCQ&RES-treated group (7C): showing intact cells of inner nuclar layer (INL) with minimal cytoplasmic vacuoles (arrow) in bipolar cells (BP). Outer nuclear layer (ONL) and outer plexiform layer (OPL) are seen (TEMx4700, scale bar 10 µm).

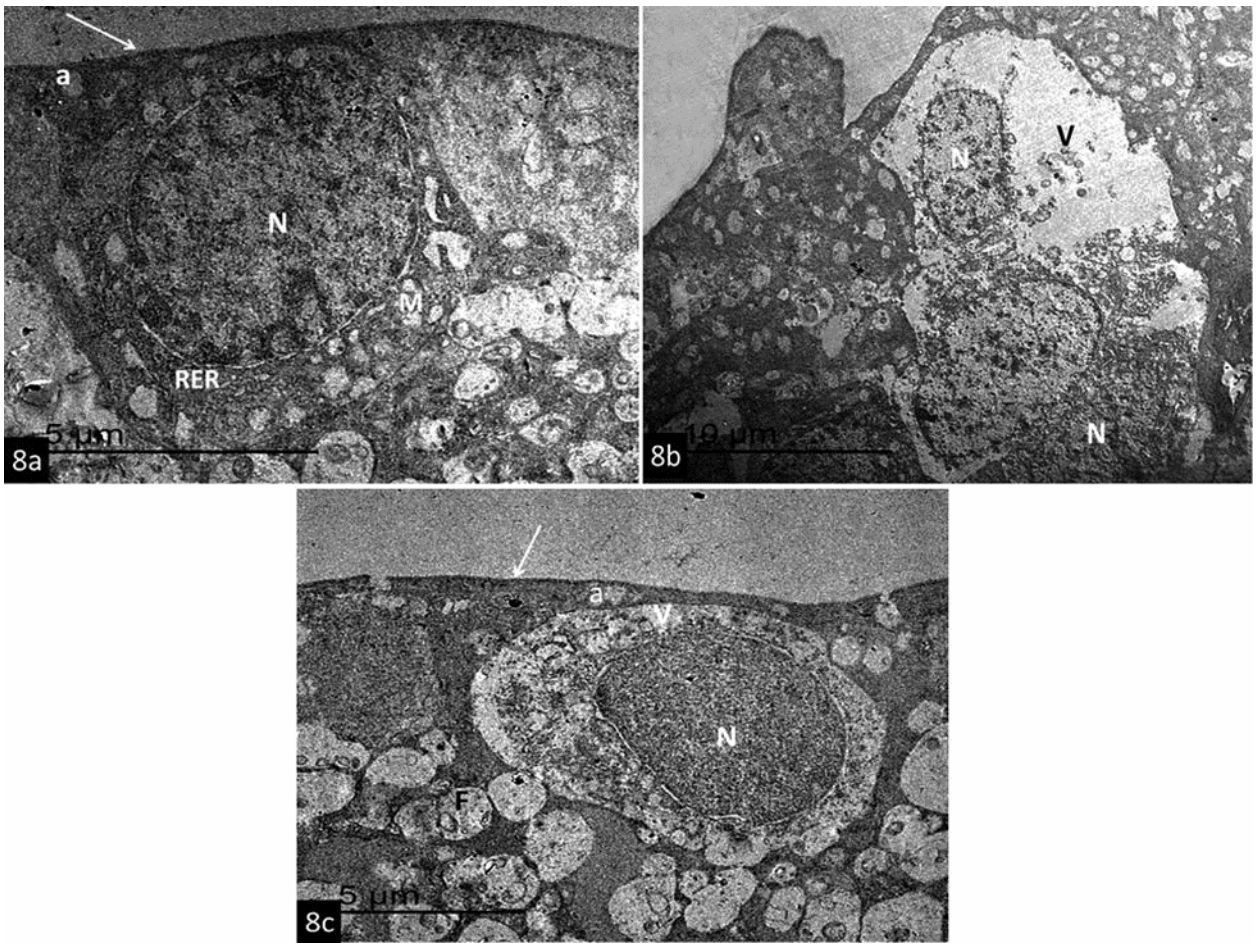

Figure 8: Electron micrographs of the ganglion cell layer of retina of control group (8a): showing a ganglion cell with oval euchromatic nucleus (N), mitochondria (M) and cisterna of rough endoplasmic reticulum (RER). Un-myelinated axons (a) of the ganglion cells were seen in the optic nerve fiber layer. The inner limiting membrane was also noticed (arrow) (TEMx26000, scale bar 5 µm). HCQ-treated group (8b): showing ganglion cells with irregular nuclei (N) and vacuolated cytoplasm (V) (TEMx10000, scale bar 10 µm). HCQ&RES-treated group (8C): showing a ganglion cell with euchromatic nucleus (N). Some vacuoles (v) are observed in the cytoplasm. Inner limiting membrane (arrow) and Nerve fibers (F) in inner plexiform layer are noticed (TEMx17000 scale bar 5 µm).

DISCUSSION

Hydroxychloroquine-induced retinopathy can be asymptomatic in the early stages, however, patients with more advanced toxicity usually complain of paracentral scotomas and night vision problems. Reading difficulties, blurring of vision, field defects, glare, light flashes, disorders of color vision and metamorphopsia (visual distortions) have been also reported[22].

Turgut and Karanfil described the experimental animal models for retinal and choroidal diseases aiming to help the researchers the choice of the most favorite models in their experimental studies; they suggested that the favorite animal for experimental retinal photoreceptor degeneration is the rat[23].

The HCQ effect on photoreceptors was evident in light microscopic findings of the current study as irregular processes with vacuolations in their outer segment and irregularly oriented inner segment, in addition to the ultrastructural findings of relatively disorganized photoreceptors´ outer segments with wide intersegment spaces and shrunken

and irregular cell bodies and nuclei of rods and cones with widening of the spaces between the cell bodies. However, the current work proved affection of other layers of the retina including diminished cell population of outer and inner nuclear layers with empty spaces between their cells and many pyknotic nuclei together with decreased number, vacuolation and congested capillaries of the ganglion cell layer were also evident. The histological findings were confirmed by the significant decrease in full retinal thickness in the morphometric study. Running in parallel to this finding, previous studies showed that patients under HCQ therapy even with no clinical signs of maculopathy show significantly lower retinal nerve fiber layer thickness measurements indicating early loss of ganglion cells[24]. Also Godinho et al. found that hydroxychloroquine causes progressive thinning of the inner retinal layers, specifically in the ganglion cell layer of the foveolar and paracentral areas[25].

Regarding HCQ effect on human retina, spectral domain optical coherence tomographies (OCT) data obtained from patients with various degrees of HCQ-Induced retinopathy suggest degeneration in HCQ retinopathy is localized to the outer retina/photoreceptor layer.[26]

Autophagy is a catabolic process in which malfunctioning proteins and organelles are disintegrated and recycled. The autophagosomeis generated for the isolation of targeted or non-specific materials, and the engulfed components are destroyed by lysosomal hydrolases throughout the maturation process. In addition to degrading proteins and organelles, autophagy is important for cellular survival since it provides energy during times of metabolic stresses[27].

According to Klouda and Stone, the retina is particularly vulnerable to oxidative stress damage because it consumes the most oxygen and has the highest polyunsaturated fatty acid content of any tissue, making it more susceptible to lipid peroxidation. In addition, the decrease in phagosome clearance can provide another explanation. The complete autophagic process can be divided into several steps, including initiation, elongation and closure, maturation of autophagosomes, fusion with lysosomes as well as breakdown and release of macromolecules back to the cytosol.[28] According to Yang et al., HCQ can inhibit autophagy by blocking the fusion of autophagosomes with lysosomes[29].

The current work proved that HCQ induced significant increase in the mTOR expression levels leading to significant inhibition of autophagy manifested by deceased expression microtubule-associated protein 1 light chain 3 (LC3B) and beclin-1. Microtubule-associated protein 1 light chain 3 (LC3B) is required for autophagosomeformation[30].

In mammalian tissues, mTOR is a fundamental inhibitor of autophagy[31]. Huang et al. provided evidence that abnormal activity of mTORC1 signaling results in RPE degeneration. Degeneration of the RPE is believed to engage in a variety of retinal degenerative disorders[32].

Dhingra et al. stated that RPE relies on LC3 family of proteins for phagocytic clearance of the daily shed photoreceptor outer segments; thus maintain cell renewal and also proved that LC3B is essential for the maintenance of normal lipid homeostasis in the RPE. Beclin 1 acts as an essential mediator of autophagy and the reduced expression of Beclin 1 reduces autophagic removal of damaged organelles[33]

The autophagy-inhibiting effect of HCQ has

attracted interest as an adjuvant for chemotherapy and radiotherapy in cancer treatment, and it has a better treatment response than chemotherapy or radiation therapy that does not inhibit autophagy.This is since cancer cells use autophagy to destroy damaged organelles and reprocess macromolecules, which serves as an internal fuel reserve in the event of nutrient scarcity[34].This autophagy inhibitory action is also considered the root of a variety of side effects, most notably a remarkable chronic systemic toxicity including retinopathy[35].

In the current work, there was also an evident decrease in are % of Bcl-2 expression in HCQ-treated group. The Bcl-2 protein is a well-known anti-apoptotic mediator[36]. Beclin 1 has been shown to interact with anti-apoptotic Bcl-2 via its BH3 domain, preventing Beclin-1 from forming the pre-autophagosomal structure and thus inhibiting autophagy[37].In addition,the current work proved that HCQ induced significantly increased expression of p62. The autophagic protein p62 is efficiently degraded by autophagy, and p62 levels could be inversely related to autophagicactivity[38].

This was confirmed by ultrastructural findings of the current study that showed an increase in the number of phagosomes in the HCQ-treated group which can be explained by the oxidative stress process induced by HCQ and proved by the significant increase in MDA, protein carbonyl, 8-OHdG and the significant decrease in the total antioxidant capacity (TAC). Reactive oxygen and nitrogen species are amongst the chief intracellular signal transducers protracting autophagy[39].

In the HCQ-treated group, there was also an apparent buildup in the levels of TNF-α and caspase-3. TNF-α is a pro-inflammatory cytokine produced by macrophages and T-cells. It is important in both inflammation and apoptosis. It changes the micro-structure and causes malfunction of the mitochondria and it also provokes ROS and NO generation thus further enhancing the inflammatory response and exacerbating the neuronal damage [40]. In addition, TNF- may cause neuronal death directly by binding to TNF receptor-1 and triggering intracellular death signaling cascades. TNF- seems to play a role in the development of inflammatory, edematous, neurodegenerative, and neovascular pathologies in the eye[41].

Furthermore, caspase-3 cleavage and activation are recognized to be eminent in apoptosis. Glutaredoxin (Grx), a ubiquitous redox molecule, regulates caspase-3 cleavage by modulating caspase-3 glutathiolation. The activity of Grx is dramatically increased by tumour necrosis factor-α[42]. Manifestations of retinal degeneration in the form of elevation of caspase-3 in parallel to other reports of its activation in rodent models of photoreceptor retinal degeneration[43].

The autophagy inhibition leads to accumulation of lipofuscin in retinal pigment epithelium by inhibitingits lysosomal storage mechanismsand preventing the recycling of all-trans-retinol. Lipofuscin accumulation is implicated in many degenerative diseases of the retina, in particular in the degeneration of photoreceptors[44].

In the current work, resveratrol induced an obvious improvement in the retinal lesions induced by HCQ in the histological and ultrastructural study through many mechanisms including antioxidant activity as proved by the significant decrease in the oxidative stress parameters MDA, protein carbonyl, 8-OHdG and the significant increase in the total antioxidant capacity (TAC). Also, resveratrol decreased

significantly the inflammatory and apoptosis mediators; caspase-3 and TNF-α in parallel to Silva et al. who considered that resveratrol is a natural anti-TNF-αmolecule[45].

Huang et al. reported that blockade of mTOR signaling pathway hindered TNF-α mRNA translation[46] Ulakcsai et al. provided evidence of resveratrol's protective action against caspase-3 activation. Resveratrol triggered autophagy by significantly decreasing mTOR expression while increasing the levels of expression of LC3B, beclin-1, and significantly decreasing the levels of expression of p62[47]. There are previous reports documenting that resveratrol can directly inhibit mTOR and then induce autophagy. Park et al. demonstrated that resveratrol suppresses mTOR by docking onto mTOR's ATP-binding pocket (i.e., it competes with ATP)[48].

Kapuy et al. discovered that inhibiting mTOR resulted in an increase in cell survival, which was accompanied by an increase in autophagicactivity[49]. In accordance, Meng et al. reported that resveratrol protects against oxidative stress mainly by (a) diminishing reactive oxygen/nitrogen species production; (b) scavenging free radicals directly; (c) Increasing the effectiveness of the endogenous antioxidant system (e.g., SOD, CAT, and GSH); (d) stimulating antioxidant molecules and the expression of associated genes implicated in mitochondrial energy biogenesis, mainly through AMPK/SIRT1/Nrf2, ERK/p38 MAPK, and PTEN/Akt signaling pathways; (e) provoking autophagy via mTOR-dependent or TFEB-dependent pathway[50].

CONCLUSION

Hydroxychloroquine is effective for the treatment of systemic disease but HCQ toxicity induces side effects including retinopathy. The current work highlighted the role of autophagy inhibition in the pathogenesis of retinopathy and proved that resveratrol can ameliorate this major problem through many mechanisms including autophagy induction mediated by mammalian target of rapamycin (mTOR) signaling pathway and also through promotion of the oxidant/antioxidant balance.

CONFLICT OF INTEREST

The authors declare that there is no conflict of interest

FUNDING DISCLOSURE

The authors declare that they did not receive funding

REFERENCES

1. **Maenpaa H, Toimela T, Mannerstrom M, et al.** Toxicity of selected cationic drugs in retinoblastomal cultures and in cocultures of retinoblastomal and retinal pigment epithelial cell lines. Neurochem Res 2004; 29: 305-311.
2. **O'Dell JR, Mikuls TR, Taylor TH, et al.** Therapies for active rheumatoid arthritis after methotrexate failure. N Engl J Med 2013; 369(4): 307-318.
3. **Meyerowitz EA, Vannier AG, Friesen MG, et al.**Rethinking the role of hydroxychloroquine in the treatment of COVID-19. FASEB J 2020; 34(5): 6027–6037.
4. **Bernstein HN.** Ocular safety of hydroxychloroquine. Ann Ophthalmol. 1991; 23(8):292-296.
5. **Yusuf IH, Sharma S, Luqmani R, et al.**Hydroxychloroquine retinopathy. Eye (Lond) 2017; 31(6): 828-845.
6. **Pandya HK, Robinson M, Mandal N, et al.**Hydroxychloroquine retinopathy: A review of imaging. Indian J Ophthalmol 2015; 63(7): 570-574.
7. **Moschos MM, Nitoda E, Chatziralli IP, et al.** Assessment of hydroxychloroquine maculopathy after cessation of treatment: an optical coherence tomography and multifocal electroretinography study. Drug Des DevelTher 2015; 9: 2993-2999.
8. **Wang Y, Catana F, Yang Y, et al.** An LCMS method

for analyzing total resveratrol in grape juice, cranberry juice, and in wine. J Agric Food Chem 2002; 50(3): 431–435.

9. **Aggarwal BB, Bhardwaj A, Aggarwal RS, et al.** Role of resveratrol in prevention and therapy of cancer: preclinical and clinical studies. Anticancer Res 2004; 24(5A): 2783–2840.
10. **Huminiecki L and Horbanczuk J.** The functional genomic studies of resveratrol in respect to its anti-cancer effects. BiotechnolAdv 2018; 36(6): 1699–1708.
11. **Sameer SK and CarlesCantó.** The molecular targets of resveratrol. Biochimica et BiophysicaActa (BBA) - Molecular Basis of Disease 2015; 1852(6): 1114-1123
12. **Tian Y, Song W, Li D, Cai L, et al.** Resveratrol As A Natural Regulator Of Autophagy For Prevention And Treatment Of Cancer. Onco Targets Ther 2019; 12: 8601-8609.
13. **Rocha-González HI, Ambriz-Tututi M, Granados-Soto V.** Resveratrol: a natural compound with pharmacological potential in neurodegenerative diseases. CNS NeurosciTher 2008; 14(3): 234-247.
14. **Radwan RR and Karam HM.** Resveratrol attenuates intestinal injury in irradiated rats via PI3K/Akt/mTOR signaling pathway. Environ Toxicol 2020; 35(2): 223-230.
15. Safety data sheet SDS. Hydroxychloroquine sulfate (CAS-No. 747-36-4), toxicological information, Fermion Oy, Koivu-Mankkaan tie 6A, FI-02200 Espoo, Finland 2015; pp: 1-10, available at: https://www.fermion.fi/globalassets/global-files/fermion/msds/hydroxychloroquine.pdf
16. **vanHerck H, Baumans V, Brandt CJWM, et al.** Orbital sinus blood sampling in rats as performed by different animal technicians: the influence of technique and expertise. Lab Animals 1998; 32: 377-386
17. **Livak KJ and Schmittgen TD.** Analysis of relative gene expression data using real-time quantitative PCR and the 2(-Delta DeltaC(T)). Method 2001; 25: 402-408
18. **Fielden MR, Werner J, Jamison JA, et al.** Retinal Toxicity Induced by a Novel β-secretase Inhibitor in the Sprague-Dawley Rat. ToxicolPathol 2015; 43(4): 581-592.
19. **Bancroft J and Layton C** .The Hematoxylin and eosin. In: Suvarna SK, Layton C and Bancroft JD editors. Theory and Practice of histological techniques. 7th ed. 2013; pp 172-214, Churchill Livingstone of Elsevier, Philadelphia.
20. **Dey P.** Basic and Advanced Laboratory Techniques in Histopathology and Cytology. 2018;Pp 149-162 Springer Nature, Gateway East, Singapore.
21. **Hayat M.** Principles and Techniques of Electron Microscopy Biological Applications. 4th ed., 2000; Pp: 70-92. Maac Millan Press, London
22. **Yusuf IH, Sharma S, Luqmani R, et al.**Hydroxychloroquine retinopathy. Eye (Lond) 2017; 31(6): 828-845.
23. **Turgut B and Karanfil FC**. Experimental Animal Models for Retinal and Choroidal Diseases. AdvOphthalmol Vis Syst 2017; 7(4): 00232.
24. **Brandao LM and Palmowski-Wolfe AM.** A possible early sign of hydroxychloroquine macular toxicity. Doc OphthalmolAdvOphthalmol 2016; 132(1): 75–81
25. **Godinho G, Madeira C, Falcão M, et al.** Longitudinal Retinal Changes Induced by Hydroxychloroquine in Eyes without Retinal Toxicity. Ophthalmic Res 2021; 64: 290-296.
26. **deSisternes L, Hu J, Rubin DL, Marmor MF.** Localization of damage in progressive hydroxychloroquine retinopathy on and off the drug: inner versus outer retina, parafovea versus peripheral fovea. Invest Ophthalmol Vis Sci 2015; 56: 34153426.
27. **Levine B and Yuan J.** Autophagy in cell death: an innocent convict? J Clin Invest 2005; 115: 2679–2688.
28. **Klouda CB and Stone WL.** Oxidative Stress, Proton Fluxes, and Chloroquine/Hydroxychloroquine Treatment for COVID-19. Antioxidants (Basel) 2020; 9(9): 894.
29. **Yang YP, Hu LF, Zheng HF, et al.** Application and interpretation of current autophagy inhibitors and activators. ActaPharmacol Sin 2013; (5): 625-35.
30. **Gao N, Wang H, Yin H, et al**. Angiotensin II induces calcium-mediated autophagy in podocytes through

enhancing reactive oxygen species levels. ChemBiol Interact 2017; 277: 110–118.

31. **Kim YC and Guan KL. mTOR**: a pharmacologic target for autophagy regulation. J Clin Invest 2015; 125(1): 25-32.
32. **Strauss O.** The retinal pigment epithelium in visual function. Physiol Rev 2005; 85(3): 845-881.
33. **Marquez RT and Xu L.** Bcl-2: Beclin 1 complex: multiple, mechanisms regulating autophagy/apoptosis toggle switch. Am J Cancer Res 2012; 2(2): 214-221
34. **Haas NB, Appleman LJ, Stein M, et al.** Autophagy Inhibition to AugmentmTOR Inhibition: a Phase I/II Trial of Everolimus and Hydroxychloroquine in Patients with Previously Treated Renal Cell Carcinoma. Clin Cancer Res 2019; 25(7): 2080-2087.
35. **Muller R.** Systemic toxicity of chloroquine and hydroxychloroquine: prevalence, mechanisms, risk factors, prognostic and screening possibilities. RheumatolInt 2021; 41(7): 1189-1202.
36. **Hata AN, Engelman JA, Faber AC.** The BCL2 Family: Key Mediators of the Apoptotic Response to Targeted Anticancer Therapeutics. Cancer Discov 2015; 5(5): 475-487.
37. **Kang R, Zeh HJ, Lotze MT, et al.** The Beclin 1 network regulates autophagy and apoptosis. Cell Death Differ 2011; 18(4): 571-580.
38. **Bjorkoy G, Lamark T, Johansen T.** p62/SQSTM1: a missing link between protein aggregates and the autophagy machinery. Autophagy 2006; 2: 138–139
39. **Filomeni G, De Zio D, Cecconi F.** Oxidative stress and autophagy: the clash between damage and metabolic needs. Cell Death Differ 2015; 22(3): 377-388.
40. **Mir M, Tolosa L, Asensio VJ, et al**. Complementary roles of tumor necrosis factor alpha and interferon gamma in inducible microglial nitric oxide generation. J Neuroimmunol 2008; 204: 101–109.
41. **Mirshahi A, Hoehn R, Lorenz K, et al.** Anti-tumor necrosis factor alpha for retinal diseases: current knowledge and future concepts. J Ophthalmic Vis Res 2012; 7(1): 39-44.
42. **Pan S and BerkBC**Glutathiolation regulates tumor necrosis factor-alpha-induced caspase-3 cleavage and apoptosis: key role for glutaredoxin in the death pathway. Circ Res 2007; 100(2): 213-219.
43. **Zeiss CJ, Neal J, Johnson EA.** Caspase-3 in postnatal retinal development and degeneration. Invest Ophthalmol Vis Sci 2004; 45(3):964-70.
44. **Blasiak J.** Senescence in the pathogenesis of age-related macular degeneration. Cell Mol Life Sci 2020; 77(5): 789-805.
45. **Silva AM, Oliveira MI, Sette L, et al.** Resveratrol as a natural anti-tumor necrosis factor-α molecule: implications to dendritic cells and their crosstalk with mesenchymal stromal cells. PLoS One 2014; 9(3): e91406.
46. **Huang HY, Chang HF, Tsai MJ, et al.** 6-Mercaptopurine attenuates tumor necrosis factor-α production in microglia through Nur77-mediated transrepression and PI3K/Akt/mTOR signaling-mediated translational regulation. J Neuroinflammation 2016; 13(1): 78.
47. **Ulakcsai Z, Bagaméry F, Vincze I, et al**. Protective effect of resveratrol against caspase 3 activation in primary mouse fibroblasts. Croat Med J 2015; 56(2): 78-84.
48. **Park D, Jeong H, Lee MN, et al.** Resveratrol induces autophagy by directly inhibiting mTOR through ATP competition. Sci Rep 2016; 6: 21772.
49. **Kapuy O, Vinod PK, Bánhegyi G**. mTOR inhibition increases cell viability via autophagy induction during endoplasmic reticulum stress - An experimental and modeling study. FEBS Open Bio 2014; 4: 704-713.
50. **Meng X, Zhou J, Zhao CN, et al** Health Benefits and Molecular Mechanisms of Resveratrol: A Narrative Review. Foods 2020; 9(3): 340.

Table (S1): Forward and reverse of the primers for mTOR, Microtubule-Associated Protein 1 Light Chain 3 (LC3B), Beclin-1 and p62 Genes and the house keeping (β-actin) gene:

Genes	Primer sequence
-mTOR	Forward:5`- GGAGCCCCTGCATGCTATGA-3` Reverse: 5`- CGGCACCATTCTTGTGCCTC-3`
- Microtubule-Associated Protein 1 Light Chain 3 (LC3B)	Forward:5`- CATGCCGTCCGAGAAGACCT-3` Reverse:5`- CCGGATGAGCCGGACATCTT-3`
- Beclin-1	Forward:5`- CAGCTCTCGTCAAGGCGTCA-3` Reverse: 5`- ATTCTTTAGGCCCCGACGCT-3`
- P62	Forward:5`- CTGAGTCGGCTTCTGCTCCA-3` Reverse: 5`- GCGGCTTCTCTTCCCTCCAT -3`
- β-actin	Forward:5`- CCACCCGCGAGTACAACCTT -3` Reverse:5`- CCCACGATGGAGGGGAAGAC -3`

Table (S2): statistical comparison among different studied groups of biochemical parameters (serum caspase-3 and tumor necrosis factor-alpha) and serum oxidative stress parameters (MDA, protein carbonyl, 8-OHdG, TAC) by one way ANOVA with Tukey HSD post-hoc test:

Group / Parameter	Negative control group	Hydroxychloroquine-treated group	Hydroxychloroquine and resveratrol-treated group	*p*-value
	Mean±SD			
Serum caspase-3 (ng/ml)	0.834±0.158	4.67±1.483[a]	1.508±0.528[b]	<0.0001*
Serum tumor necrosis factor-alpha (TNF-α) (pg/g)	32.30±6.28	77.62±11.28[a]	39.53±10.94[b]	<0.0001*
Oxidative stress parameters				
MDA (nmol/ml)	5.09±1.33	23.75±7.65[a]	9.80±3.45[b]	<0.0001*
protein carbonyl (nmol/ml)	0.15±0.049	0.42±0.097[a]	0.18±0.032[b]	<0.0001*
8-OHdG (ng/ml)	0.16±0.035	0.43±0.086[a]	0.20±0.033[b]	<0.0001*
TAC (mmol/l)	1.93±0.12	1.13±0.22[a]	1.53±0.55[a, b]	<0.0001*

SD: standard deviation *: significant
a: versus control b: versus hydroxychloroquine -treated group

Table (S3): statistical comparison among different studied groups of mTOR, Microtubule-Associated Protein 1 Light Chain 3 (LC3B), Beclin-1and P62 Genes expression by one way ANOVA with Tukey HSD post-hoc test

Group / Gene expression	Negative control group	Hydroxychloroquine-treated group	Hydroxychloroquine & resveratrol-treated group	*p*-value
	Mean±SD			
- mTOR	1.00±0.00	3.17±0.98[a]	1.16±0.23[b]	<0.0001*
- Microtubule-Associated Protein 1 Light Chain 3 (LC3B)	1.00±0.00	0.73±0.12[a]	1.10±0.14[b]	<0.0001*
-Beclin-1	1.00±0.00	0.69±0.15[a]	1.14±0.34[b]	<0.0001*
-p62	1.00±0.00	2.22±0.21[a]	1.19±0.28[b]	<0.0001*

SD: standard deviation *: significant
[a]: versus tramadol-treated group [b]: versus alcohol-treated group

Table (S4): statistical comparison among different studied groups of the full retinal thickness and the area percentage (area %) of positive immunoreaction for Bcl-2 by one way ANOVA with Tukey HSD post-hoc test:

Group / Parameter	Negative control group	Hydroxychloroquine-treated group	Hydroxychloroquine& resveratrol-treated group	*p*-value
	Mean±SD			
-Full retinal thickness	149.64±12.30	118.31±9.66[a]	135.90±9.03[a, b]	<0.0001*
- Area % of positive immunoreaction for Bcl-2	0.347±0.512	0.151±0.0338[a]	0.292±0.0808[b]	<0.0001*

SD: standard deviation *: significant
[a]: versus negative control [b]: versus hydroxychloroquine -treated group

Citation:
Abdelfadeel, K., Abdel Hamid, O. I., Alazouny, Z. Resveratrol Ameliorates Hydroxychloroquine-Induced Retinopathy by Autophagy Induction: Molecular and Morphological Evidences. *Zagazig University Medical Journal*, 2022; (4227-4249): -. doi: 10.21608/zumj.2022.132439.2546